Efficient and Rigorous 3D Model for Optical Lithography Simulation

Kevin D. Lucas[1,3], Hiroyoshi Tanabe[2], Chi-Min Yuan[1] and Andrzej J. Strojwas[3]

[1]Advanced Products Research & Development Lab, Motorola Inc., Austin TX 78721, USA
[2]Opto-Electronics Research Lab, NEC Corporation, Kawasaki, Kanagawa 216, Japan
[3]Electrical & Computer Engin. Dept., Carnegie Mellon Univ., Pittsburgh, PA 15213, USA

Abstract

A new workstation-based rigorous model for 3D vector lithography simulation is introduced. The model extends a successful 2D lithography model, and has been applied to the simulation of 3D photomasks. The theory behind the new model is presented, and examples are given of the model's results and computational efficiency. The procedures for extending the model to the simulation of 3D optical alignment, metrology and photoresist bleaching problems are also given.

1. Introduction

Decreasing dimensions and increasing non-planarity of devices are creating complicated problems for the optical lithography process in semiconductor manufacturing. The large cost and time necessary for experiments make rigorous photolithography simulation increasingly cost effective in the solution of these problems. These problems include the modeling of realistic corners, contacts, vias, alignment marks and defects. We are presenting a new vector 3D model which runs quickly on common engineering workstations. This model has been implemented into a simulator, METROPOLE-3D, for the study of 3D photomasks.

The basis for this work was the extension of the fast and rigorous 2D *waveguide method,* a spatial frequency solution to Maxwell's equations[1]. The 2D method was previously implemented into a simulator, METROPOLE, and applied to the study of optical alignment and metrology[1], substrate bleaching[2] and phase shifting masks[3]. A major benefit of the *waveguide method* is its ability to simultaneously solve for all incoherent incoming light orders. Traditional models must repeat their simulations for each of these orders, which in 3D modeling may number in the hundreds.

2. 3D Theory

The potential for a 3D waveguide theory using vector potentials was shown by Tanabe[5]. The E and H fields are described using vector potential A and scalar potential ϕ as: $H = \nabla \times A$ and $E = ikA - \nabla\phi$. Inserting into Maxwell's equations provides the characteristic equation:

$$\nabla^2 A + k^2 \varepsilon A - \nabla(\nabla \bullet A) + ik\varepsilon\nabla\phi = 0 \cdot$$

Because of gauge freedom, the vector and scalar potentials can be changed simultaneously by $A \rightarrow A - \nabla\Lambda$ $\phi \rightarrow \phi - ik\Lambda$ and observables E and H are unaffected.

Implementing the Lorentz gauge, which provides $\nabla \bullet A = ik\varepsilon\phi$, allows writing the characteristic equation as $\nabla^2 A + k^2 \varepsilon A - \nabla(\log\varepsilon)(\nabla \bullet A) = 0$.

Tanabe used the *waveguide method* approximation where non-planar structures are described by (often thin) layers in which the dielectric function is constant vertically (*z*-direction) but varies in the horizontal *x* and *y* directions (See Figure 1). This allows simplifying the *z* component of the characteristic equation in a layer to be $\nabla^2 A_z + k^2 \varepsilon A_z = 0$.

However, gauge freedom still exists. This allows using the transformation $\frac{\partial \Lambda}{\partial z} = A_z$ to set $A_z = 0$. Significantly, the characteristic equation, which is Maxwell's equations in vector potential form in each layer, is reduced to two coupled partial differential equations:

$$\nabla^2 A_x + k^2 \varepsilon A_x - \frac{\partial}{\partial x}\log\varepsilon\left(\frac{\partial A_x}{\partial x} + \frac{\partial A_y}{\partial y}\right) = 0 \qquad \nabla^2 A_y + k^2 \varepsilon A_y - \frac{\partial}{\partial y}\log\varepsilon\left(\frac{\partial A_x}{\partial x} + \frac{\partial A_y}{\partial y}\right) = 0$$

This formulation has only two variables to be solved for as opposed to three for traditional methods. In this work, we solve these equations, beginning by using the relations, $A_x = f(x,y)Z(z)$ $A_y = g(x,y)Z(z)$ and $Z(z) = C \cdot exp(\alpha z) + C' \cdot exp(-\alpha z)$.

Substituting truncated Fourier series for ε, log ε, *f(x,y)* and *g(x,y)*, such as

$$f(x,y) = \sum_{l=-N}^{N}\sum_{m=-N}^{N} B_{l,m}\ exp\left(i2\pi\{b_1 lx + b_2 my\}\right) \qquad g(x,y) = \sum_{l=-N}^{N}\sum_{m=-N}^{N} D_{l,m}\ exp\left(i2\pi\{b_1 lx + b_2 my\}\right)$$

where N is the # of approximating orders, we create a coupled eigenvalue problem for each layer which may be solved for the α, *B* and *D* coefficients

$$[J_1]B + [J_2]D = -\alpha^2 B \quad \text{and} \quad [J_3]D + [J_4]B = -\alpha^2 D \quad \text{or} \quad \begin{bmatrix} J_1 & J_2 \\ J_4 & J_3 \end{bmatrix}\begin{bmatrix} B \\ D \end{bmatrix} = -\alpha^2 \begin{bmatrix} B \\ D \end{bmatrix}$$

where each J_i is a full complex matrix of size $4N^2$ x $4N^2$.

3. Boundary Conditions

The *C* and *C'* coefficients still need to be calculated. These can be obtained from the continuity of parallel components of the *E* and *H* fields between layers. Inside any layer *j*, we are able to write A_x and A_y, using $\Psi_{l,m} = exp\left(i2\pi\{b_1 lx + b_2 my\}\right)$, at a relative *z* position (See Figure 1), as

$$A_x^j = \sum_{h=1}^{2N}\left[C_h^j \cdot exp\left(\alpha_h^j (z - z_j)\right) + C_h^{j\prime} \cdot exp\left(-\alpha_h^j (z - z_j)\right)\right]\sum_l\sum_m B_{h,l,m}^j \Psi_{l,m}$$

$$A_y^j = \sum_{h=1}^{2N}\left[C_h^j \cdot exp\left(\alpha_h^j (z - z_j)\right) + C_h^{j\prime} \cdot exp\left(-\alpha_h^j (z - z_j)\right)\right]\sum_l\sum_m D_{h,l,m}^j \Psi_{l,m}$$

In layer 0, where $\Omega_{l,m}^0 = ik\sqrt{\varepsilon - (lb_1\lambda)^2 - (mb_2\lambda)^2}$, A_x and A_y are given by:

$$A_x^0 = \sum_l\sum_m \{X_{l,m}^0 e^{-z\Omega_{l,m}^0} + a_{x(l,m)} e^{z\Omega_{l,m}^0}\}\Psi_{l,m} \qquad A_y^0 = \sum_l\sum_m \{Y_{l,m}^0 e^{-z\Omega_{l,m}^0} + a_{y(l,m)} e^{z\Omega_{l,m}^0}\}\Psi_{l,m}$$

In the substrate A_x and A_y are defined relative to the substrate depth, z_s, as:

$$A_x^S = \sum_l\sum_m \{X_{l,m}^S e^{ik(z-z_s)\sqrt{\varepsilon_s - (lb_1\lambda)^2 - (mb_2\lambda)^2}}\}\Psi_{l,m} \quad A_y^S = \sum_l\sum_m \{Y_{l,m}^S e^{ik(z-z_s)\sqrt{\varepsilon_s - (lb_1\lambda)^2 - (mb_2\lambda)^2}}\}\Psi_{l,m}$$

At the interface of layers 0 and 1, we impose the boundary conditions and eliminate X^0 and Y^0 to obtain: $G^1\begin{bmatrix} C^1 \\ C'^1 \end{bmatrix} = R\begin{bmatrix} a_x \\ a_y \end{bmatrix}$ which can be written as $T^0\begin{bmatrix} C^1 \\ C'^1 \end{bmatrix} = \begin{bmatrix} a_x \\ a_y \end{bmatrix}$.

We use boundary conditions between layers j and $j+1$ to relate C coefficients $G^j \begin{bmatrix} C^j \\ C'^j \end{bmatrix} = G^{j+1} \begin{bmatrix} C^{j+1} \\ C'^{j+1} \end{bmatrix}$ or $\begin{bmatrix} C^j \\ C'^j \end{bmatrix} = T^j \begin{bmatrix} C^{j+1} \\ C'^{j+1} \end{bmatrix}$ and we use boundary conditions between the last layer and the substrate to write the expression:

$G^q \begin{bmatrix} C^q \\ C'^q \end{bmatrix} = H \begin{bmatrix} X^S \\ Y^S \end{bmatrix}$ or $\begin{bmatrix} C^q \\ C'^q \end{bmatrix} = T^q \begin{bmatrix} X^S \\ Y^S \end{bmatrix}$. H and T have size $16N^2$ x $8N^2$. For a structure with q layers, we combine T matrices to obtain $U^j = T^j T^{j+1} T^{j+2} \ldots T^q$ allowing us to write $\begin{bmatrix} X^S \\ Y^S \end{bmatrix} = \left(U^0\right)^{-1} \begin{bmatrix} R_1 \\ R_2 \end{bmatrix}$ and $\begin{bmatrix} C^j \\ C'^j \end{bmatrix} = U^j \begin{bmatrix} X^S \\ Y^S \end{bmatrix}$ where R contains the illumination information, X^S & Y^S are the amplitudes of transmitted light and X^0 & Y^0 are the amplitudes of light reflected from the structure. Thus, for modeling 3D photomasks we can compute X^S and Y^S, for 3D alignment and optical metrology we can compute X^0 & Y^0 from C^1 and C'^1 . and for modeling 3D photoresist bleaching, the internal light amplitudes in layers can be known by using the C and C' of a layer to solve for A_x and A_y.

4. Results

The model was implemented into a photomask simulator, METROPOLE-3D, which runs on engineering workstations. We have simulated examples of 3D binary and phase shifting masks for 1X and 5X reduction imaging systems. Rigorous simulation is necessary for masks with small structure sizes (approaching the wavelength of illuminating light) and for masks with vertical topography. These masks have light scattering effects which are not taken into account by approximate, scalar simulators. To verify the results of our model, we compared aerial images generated by METROPOLE-3D versus experimental images and those generated by a scalar model, SPLAT[5](See Figure 2). The imaging system had a 5X reduction factor, I-line illumination (λ=0.365 micron), a numerical aperture of 0.6, and a partial coherence of 0.6. The images are cross sections for isolated contact openings of 0.49 and 0.39 microns, after reduction, in a 10% transmission embedded attenuating phase shifting mask. The experimental aerial images were provided by SEMATECH. As can be seen, with the larger 0.49 micron opening, the results of METROPOLE-3D and the scalar model both match the experimental data well. However, for the 0.39 micron opening, where light scattering effects are more pronounced, only our rigorous vector model is able to accurately predict the experimental light intensity results. Modeling of these small mask features is important for the quick and accurate design of masks in the critical layers of next generation devices. We also implemented theoretical checking routines for comparing the model's results against the conservation of energy and reciprocity theorems. Our model's error from the theoretical predictions is very slight, typically much less than 1%.

5. Run Time and Memory Usage

Traditional workstation-based rigorous lithography models may take days to complete complex simulations. The run time of our model on an IBM RS6000 model 550 workstation is typically under a few hours for non-symmetric simulations. Simulations of fully symmetric structures typically run in under an hour[6]. The memory usage is also moderate

for today's desktop workstations, typically using less than 120MB.

6. Summary

Using a vector potential extension to an existing 2D electromagnetic solution method, we have created a new rigorous 3D lithography model. This model has been implemented in a photomask simulator for engineering workstations and has been shown to run quickly and accurately. In addition, the model is easily extendable to the efficient solution of other non-planar 3D lithography problems in optical alignment, metrology and photoresist bleaching.

References

[1] C. M. Yuan, A. J. Strojwas. *Proc. of SPIE Microlithography* Vol. 1264, 1990.
[2] K. D. Lucas, C. M. Yuan, A. J. Strojwas. *SISDEP IV,* 1991.
[3] K. D. Lucas, A. J. Strojwas. *Proc. of SPIE Microlithography* Vol. 1809, 1992.
[4] H. Tanabe. *Proc. of SPIE Microlithography* Vol. 1674, 1992.
[5] K. K. H. Toh, A. R. Neureuther. *Proc. of SPIE Microlithography* Vol. 1463, 1991.
[6] K. D. Lucas, H. Tanabe, A. J. Strojwas. *Proc. of SPIE Microlithography* Vol. 2440, 1995.

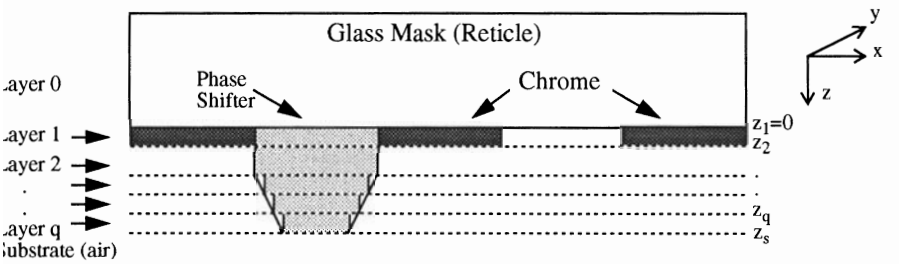

Figure 1. 2D cross section of multiple layer approximation for slanted shifter phase shifting mask. The approximation is valid if the distance errors introduced are much less than the wavelength of light.

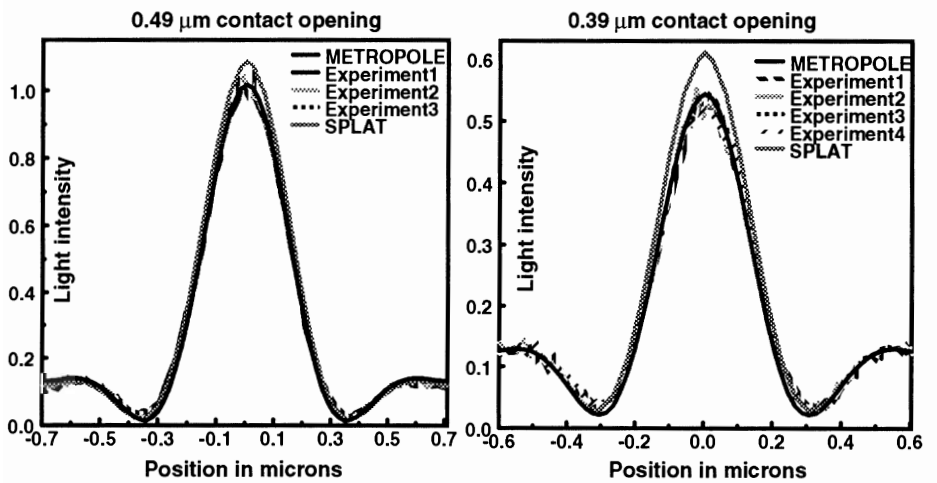

Figure 2. Cross sections of aerial images of 0.49 μm and 0.39 μm contacts in 10% attenuated PSM.